Smart Materials and Structures

PAPER • **OPEN ACCESS**

Ionic polymer–metal composite (IPMC) as a flexible capacitor: a COMSOL multiphysics study

To cite this article: Liya Napollion *et al* 2025 *Smart Mater. Struct.* **34** 085020

OPEN ACCESS
IOP Publishing
Smart Materials and Structures
Smart Mater. Struct. **34** (2025) 085020 (11pp)
https://doi.org/10.1088/1361-665X/adf929

Ionic polymer–metal composite (IPMC) as a flexible capacitor: a COMSOL multiphysics study

Liya Napollion, Jongcheol Lee, John Albert Faccinto and Kwang J Kim*

Active Materials and Smart Living (AMSL) Laboratory, Department of Mechanical Engineering, University of Nevada Las Vegas (UNLV), 4505 S Maryland Pkwy, Las Vegas, NV 89154, United States of America

E-mail: kwang.kim@unlv.edu

Received 6 April 2025, revised 25 July 2025
Accepted for publication 7 August 2025
Published 19 August 2025

Abstract

This work investigates the behavior of ionic polymer–metal composite (IPMC) capacitors, which are promising for flexible energy storage applications due to the mechanical softness and stability in aqueous environments. A physics-based modeling framework was developed to reveal the inner workings of IPMC-based capacitors, comprising solid-state electrolytes, platinum electrodes, and coupled ion transport and electrostatic interactions. The model, implemented in COMSOL multiphysics, was qualitatively validated by comparing simulated and experimental cyclic voltammogram (CV) curves, focusing on capturing capacitive behavior and the magnitude of the current values over the scanned voltage range. To explore the device performance characteristics, the effects of the voltage scan rate and the presence of microcracks in the electrodes on capacitor behavior were investigated using the model. Microcracks, which often result from fabrication processes or continuous bending, pose challenges in predicting device performance. Simulations showed that reducing the scan rate from 0.1 to 0.015 V s^{-1} increased the specific capacitance from approximately 0.9–2.9 mF g^{-1}. Additionally, the introduction of thousands of randomly distributed microcracks, based on experimentally observed densities, led to only a modest capacitance reduction (∼4.5%), indicating that IPMC capacitors are tolerant to minor structural imperfections. These findings demonstrate the utility of the modeling framework in evaluating structural and operational factors that influence IPMC capacitor behavior. Unlike previous modeling studies focused on actuation and sensing, this work introduces a dedicated simulation framework for IPMC capacitor modeling, incorporating the effects of electrode microcracks to potentially support predictive design in flexible energy storage systems.

Keywords: ionic polymer–metal composite, flexible, capacitors, COMSOL, multiphysics

* Author to whom any correspondence should be addressed.

1. Introduction

Ionic polymer–metal composites (IPMCs) are advanced materials composed of an ionic polymer membrane and electrodes bonded to both sides of the membrane. The membrane consists of fixed anionic groups covalently attached to the polymer backbone, balanced by mobile cations in water solutions [1, 2]. These materials have garnered significant interest in various applications because of their unique electromechanical properties [3–5]. Most research to date has focused on utilizing IPMC materials as actuators and sensors [4, 6]. In addition, there has been research on the potential of IPMC materials for electrical energy harvesting [7–9], where they convert mechanical energy into electrical energy.

Recently, there has been growing interest and research in utilizing IPMC as planar and flexible capacitors for energy storage in wearable and soft electronic system, such as wearable biosensors, soft robotics, and implantable electronics [10, 11]. When an external electric potential is applied to IPMC electrodes, mobile cations redistribute and accumulate near the electrode-membrane interface, forming electrical double layers (EDLs) at both electrodes [2, 3]. This mechanism is electrochemical in nature and distinct from conventional dielectric capacitors, which rely on electronic charge separation across a dielectric material between rigid electrodes. Reported specific capacitance values for IPMCs range from approximately 20–45 mF cm^{-2} under hydrated conditions, depending on ion type, membrane, and mechanical strain [9, 12, 13]. Although these values are lower than those of CNT-based supercapacitors, which often exceed 200 F g^{-1} or 1 F cm^{-2} [14], IPMCs still provide sufficient capacitance for low-power, flexible applications.

Compared to dielectric and CNT-based capacitors, IPMCs offer several practical advantages including stable operation in hydrated or underwater environment, inherent mechanical softness, and potential for multifunctionality such as mechano-electrical self-charging during deformation [9]. Despite these strengths, several challenges remain for real-world implementation. Notably, long-term performance degradation caused by mechanical stress or structural defects, such as microcrack formation in metal electrodes, can compromise ionic transport and charge storage. Furthermore, there is limited understanding of how such degradation mechanisms affect electrochemical performance, and few predictive modeling frameworks exist to assess their impact.

The formation of microcracks in the metal electrodes of IPMCs can significantly impact their capacitive behavior by disrupting the physical and electrochemical integrity of the electrode-membrane interface. Increased surface resistance due to cracks can disrupt the uniform distribution of the electric field, impede efficient cation migration, and thus reduce charge accumulation at the electrode-membrane interfaces [15, 16]. Since the formation of EDLs at the interface is essential for charge storage in IPMC capacitors, any interruption in ionic access to electrode sites directly reduces the effective capacitance [17, 18]. For instance, Tiwari and Kim showed that controlled introduction of surface cracks or perforations may enhance capacitance by increasing interfacial area and improving ion accessibility under hydrated conditions [19]. While prior studies have investigated the impact of microcracks on actuation and mechanical integrity [16], the impact of tensile loading on electrochemical performance [20], the influence of crack geometry on actuation behavior through modeling [21], and capacitive behaviors upon IPMC bending [12], a comprehensive modeling approach that considers microcracks and tensile loading in relation to IPMC capacitance remains underexplored. Therefore, modeling the combined effects of microcracks and tensile loading on capacitance can provide insights for designing durable and high-performance IPMC-based capacitors.

The primary objective of this work is to establish a theoretical modeling framework that captures the capacitive behavior of IPMCs under the influence of microcracks. COMSOL multiphysics is selected for its capability to couple multiple physical phenomena, such as ion transport, electrostatics, and solid mechanics, within a single unified framework. While the details of the physics used and model geometry, and the assumptions and limitations from model simplifications are provided in the following subsection (section 2.3), we briefly note here that a two-dimensional (2D) geometry was used to model the IPMC (figure 1), and that porous electrode surfaces and complex membrane-electrode interface structures, often observed in electroless plating fabrication processes [2, 22], were not considered due to computational cost. The model is applied to evaluate the effect of rectangular-shaped microcracks on the electrochemical performance of IPMCs as an exemplar study, particularly their influence on ion distribution, current response, and specific capacitance. The modeling framework and associated physics are described in the materials and methods section, followed by simulation results of electrochemical behaviors and its comparison with experimental data in the Results and discussion section. The influence of the microcracks and tensile loading is then explored as a case study. We hypothesize that the presence of microcracks in the electrode layers of IPMCs alters ion transport and local charge distribution but does not significantly reduce overall capacitive performance under typical operational conditions. This work provides a foundation for understanding how microcracks affect capacitive behavior and offers insights into the durability of IPMC-based capacitors, supporting their development for flexible, low-power, and stable energy applications.

2. Materials and methods

2.1. IPMC fabrication and scanning electron microscopy (SEM)

The IPMC fabrication process and SEM procedure have been described in detail in previous publications [12, 20, 23]. Briefly, a surface roughened Nafion^{TM} 117 membrane was immersed in platinum salt hydrate ($Pt[(NH_3)_4]Cl_2{\cdot}H_2O$) solution for 4 h, and platinum electrodes were deposited through electroless plating using $NaBH_4$. The composite underwent

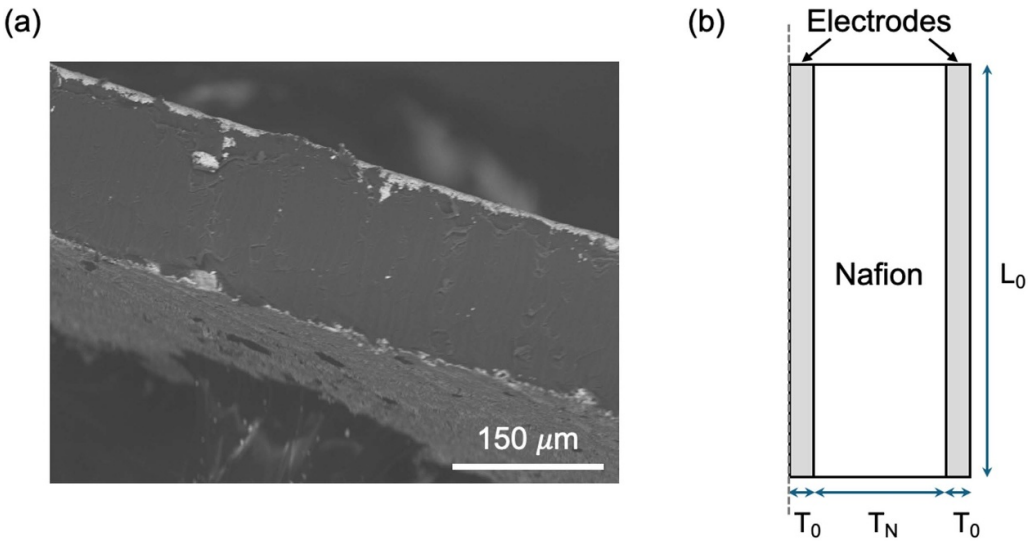

Figure 1. Scanning electron micrograph of a cross-sectioned ionic polymer–metal composite (IPMC) (a) and a schematic of the IPMC model (b). The L_0, T_0, and T_N represent the length of the IPMC, thickness of the electrode, and thickness of the Nafion^{TM}, respectively.

further plating using hydrazine. The composites were cleaned using 0.5 M H_2SO_4 and deionized water between steps. The final IPMC films were cut into 50 mm × 10 mm strips for electrical property measurements. For scanning electron micrograph, an IPMC strip was cross-sectioned using a razor blade and imaged using a Hitachi TM3030 at an accelerating voltage of 15 keV (figure 1(a)).

2.2. Cyclic voltammetry measurement

Cyclic voltammogram (CV) of the fabricated IPMC strip was recorded using a VoltaLab PGZ-402 potentiostat and the VoltaMaster 4 software. The strip was secured using a clamp with copper foil-taped contacts and placed in water. The copper contacts are connected to alligator clips and cables leading to the potentiostat. The potential was swept from −200 mV to 350 mV at scan rates of 0.015, 0.05, and 0.1 V s^{-1} at room temperature using a two-electrode system. Additional CV curves were measured under applied loads of 62 g, 162 g, and 262 g placed under the IPMC strip. The detailed experimental setup is described in previous work [20].

2.3. IPMC modeling in COMSOL multiphysics

The capacitive behavior of IPMCs was modeled using COMSOL multiphysics 6.2, a simulation platform capable of solving coupled multiphysics, involving electrostatics, ion transport, and mechanical deformation across multiple domains [24, 25]. In this framework, variables from one physics interface were constrained or driven by outputs derived from the preceding interface. This interdependence ensures that the outputs of one module, such as electric potential or current density, serve as boundary conditions or source terms in subsequent physics, thereby maintaining physical consistency across the model.

While the specific model geometry, domain setup, meshing strategy, and boundary conditions are detailed in the following subsections (sections 2.3.1–2.3.3), this section outlines the overall modeling architecture and coupling strategy across multiple physics interfaces. Four physics interfaces were applied: electric currents, coefficient form PDE (Electrostatics), electroanalysis, and solid mechanics. This combination was chosen based on their demonstrated utility in simulating electrochemical and mechanical behavior in IPMCs and related systems. Specifically, electric currents and coefficient form PDE have been used in IPMC actuation modeling by Pugal *et al* [25], electroanalysis is a standard interface for simulating cyclic voltammetry and other electrochemical processes, and solid mechanics enables simulation of externally applied mechanical stress. The simulation begins with the electric currents physics interface, which solves the electric potential, current density, and electric field in IPMC electrode domains (figure 1(b)). These outputs are then utilized by the coefficient form PDE (Electrostatics) physics interface to determine the electrostatic potential in the membrane domain using the previously solved electric potential as the input. In parallel, the electroanalysis physics interface uses the solved electric field and current density to analyze ion migration, diffusion, and electrochemical reactions, yielding ion concentration and total current density. Solid mechanics is used to impose mechanical loading, to examine its influence on electrochemical behavior. The physics interfaces are coupled through shared variables and boundary conditions, enabling interactions between physical domains.

2.3.1. IPMC model geometry and domain setup. The IPMC model was created through COMSOL multiphysics 6.2. A 2D Axisymmetric component was chosen to balance the need to capture essential physical phenomena with computational manageability. A 2D model of an IPMC strip was created,

Table 1. Parameters used in COMSOL modeling. The scan rate marked (*) is a representative value; multiple scan rates were studied.

Name	Value	Unit
Hydrogen ion diffusion concentration (D_A)	9.36×10^{-10}	$m^2\ s^{-1}$
Chlorine ion diffusion concentration (D_B)	2×10^{-10}	$m^2\ s^{-1}$
Reaction rate (K_0)	1.00×10^{10}	—
Electrode radius (re)	10	mm
Reference exchange current density ($i_{0,\,ref}$)	2000	$A\ m^{-2}$
Double layer capacitance (C_{dl})	0.2	$F\ m^{-2}$
Start potential ($E_{vertex\ 1}$)	−0.2	V
Switch potential ($E_{vertex\ 2}$)	0.35	V
Initial concentration at electrode (c_{B_0})	1.73×10^{-7}	$mol\ m^{-3}$
Bulk concentration (c_{bulk})	2000	$mol\ m^{-3}$
Volumetric scan rate (scan)	0.015*	$V\ s^{-1}$
Faraday's constant (F)	96 485	$C\ mol^{-1}$
Dielectric permittivity (epsilon)	3	$mF\ m^{-1}$

Table 2. Material properties used in COMSOL modeling.

Name	Nafion™	Platinum	Units
Young's modulus (E)	260	168	MPa
Poisson's ratio (ν)	0.4	0.38	—
Density (ρ)	2200	21 450	$kg\ m^{-3}$
Relative permittivity	2	1	—
Thermal conductivity	0.25	71.6	$W\ (m{\cdot}K)^{-1}$
Activation energy (dE)	1.2	—	eV
Diffusion coefficient	7×10^{-11}	—	$m^2\ s^{-1}$
Transport number	1	—	—
Activity dependence (f_{cl})	1	—	—
Electric conductivity	—	8.9×10^6	$S\ m^{-1}$
Electrolyte conductivity	0.041	0.041	$S\ cm^{-1}$

as shown in figure 1. The length of the IPMC strip (L_0), the thickness of the electrodes (T_0), and the thickness of the Nafion™ (T_N) were set to 50 mm, 0.0085 mm, and 0.183 mm, respectively. Other parameters used are listed in table 1, based on previous studies by Swain *et al* and Chinnasa *et al* [21, 26]. The electrodes were modeled as non-porous platinum electrodes to simplify the complex interaction between the membrane and electrodes for computation efficiency. The material properties of the Nafion™ 117 membrane and platinum electrode used are provided in table 2. The model was meshed using COMSOL's physics-controlled mesh generation with a normal element size, which automatically adjusts the mesh based on geometric features and boundary conditions of the applied physics interfaces, enhancing computation efficiency.

2.3.2. Physics interfaces

Electric currents physics

Electric currents physics interface was applied to the two thin platinum electrodes in the IPMC to compute the electric potential, electric field, and current density within the electrode domain. This physics interface uses the following equations, which represent current conservation (equation (1)), a generalized form of Ohm's law (equation (2)), and the relationship between electric field and potential (equation (3)):

$$\nabla \cdot J = Q_{j,v} \tag{1}$$

$$J = \sigma E + \frac{\partial D}{\partial t} + J_e \tag{2}$$

$$E = -\nabla V \tag{3}$$

where $J[A\,m^{-2}]$ is current density, $Q_{j,v}[A\,m^{-3}]$ is current source density, $\sigma[S\,m^{-1}]$ is electrical conductivity, $E[V\,m^{-1}]$ is electric field, $D\,[C\,m^{-2}]$ is electric displacement field, $J_e\,[A\,m^{-2}]$ is external current density, and $V[V]$ is electric potential. The electric potential (V) is the dependent variable in this physics. In our IPMC simulation, there is no external current density or volumetric current source, so both $Q_{j,v}$ and J_e are set to zero by default in COMSOL, as no boundary conditions for those were applied. The voltage is applied to the outer edge of the left electrode domain using the electric potential boundary condition, and the outer edge of the right electrode domain is grounded. The remaining boundaries are electrically insulated. The electric potential interaction between the electrodes and the Nafion™ membrane is described using Dirichlet boundary condition in Coefficient Form PDE physics interface.

Coefficient form PDE physics (electrostatics physics)

Coefficient Form PDE physics interface was applied to describe the Poisson's equation, which describes the potential and space charge density in the polymer membrane domain [25]. For this purpose, the unit of the dependent variable quantity was set to V, and the unit of the Source term quantity was set to $C\,m^{-3}$.This physics interface includes multiple coefficients that represent material properties and a source term describing the migration of species, but it is simplified as shown below by setting unrelated coefficients, such as absorption, mass, damping, and flux related terms (e_a, d_a, a, a, β, and γ), to zero:

$$\nabla \cdot (-c\nabla u) = f \tag{4}$$

where u is the dependent variable, and f is the source term. The variable u is the electric potential in our model. The coefficient c was set to epsilon, which is the dielectric permittivity, and the source term f was set to $F * (c_{bulk} - c_{B_0})$, which corresponds to the charge density (see table 1).

The electric potentials at the electrode-membrane interfaces from the Coefficient Form PDE and electric currents physics interfaces are coupled using a Dirichlet boundary condition. The 'Prescribed value of u' is set to 'V', which is the dependent variable in the electric currents physics interface. The Coefficient Form PDE physics interface with these settings can be replaced by the electrostatics physics interface in the AC/DC module in later versions of COMSOL. Therefore, this physics interface is referred to as electrostatics from this point forward.

Electroanalysis

Electroanalysis physics interface describes the diffusion and migration of ions and the electrochemical reaction driven by an applied potential, yielding the ion concentration and total

current density in the membrane domain. Several fundamental equations used in this physics interface are shown below:

$$\frac{\partial c_j}{\partial t} + \nabla \cdot J_j + u \cdot \nabla c_j = R_j \tag{5}$$

$$J_j = -D_j \nabla c_j \tag{6}$$

where $c_i \left[\mathrm{mol\,m^{-3}}\right]$ is the concentration of species i, $J_i \left[\mathrm{mol\,m^{-2} \cdot s}\right]$ is the ionic flux, $u \left[\mathrm{m\,s^{-1}}\right]$ is the velocity, $R_i \left[\mathrm{mol\,m^{-3} \cdot s}\right]$ is the source term from reactions, and $D_i \left[\mathrm{m^2\,s^{-1}}\right]$ is the diffusion coefficient. A no flux boundary condition was added by default to prevent species flow out of the membrane domain, and a concentration boundary condition was added to set the initial concentration of the species at the right membrane-electrode interface.

To incorporate the reaction at the electrode surface, an electrode surface boundary condition was added. In this boundary condition, the total current density is given by equation (7):

$$i_{\mathrm{total}} = \sum_m i_{\mathrm{loc},m} + i_{\mathrm{dl}} \tag{7}$$

where $i_{\mathrm{total}} \left[\mathrm{A\,m^{-2}}\right]$ is the total current density, $i_{\mathrm{loc},m} \left[\mathrm{A\ m^{-2}}\right]$ is the local current density for a reaction m, and $i_{\mathrm{dl}} \left[\mathrm{A\ m^{-2}}\right]$ is the electric double layer current density.

The local current density from a redox reaction is modeled by the Butler–Volmer equation:

$$i_{\mathrm{loc},m} = i_0 \left[\exp\left(\frac{a_a F \eta}{RT}\right) - \exp\left(\frac{\alpha_c F \eta}{RT}\right)\right] \tag{8}$$

where $i_0 \left[\mathrm{A\,m^{-2}}\right]$ is the exchange current density, α_a and α_c are the anodic and cathodic transfer coefficients, respectively, F is Faraday constant, $\eta \left[\mathrm{V}\right]$ is the overpotential, R is the universal gas constant, and $T \left[\mathrm{K}\right]$ is absolute temperature. The overpotential (η), defined as the difference between the electrode potential relative to the electrolyte ($E_{\mathrm{ct}} \left[\mathrm{V}\right]$) and the equilibrium potential ($E_{\mathrm{eq}} \left[\mathrm{V}\right]$), is expressed as follows:

$$\eta = E_{\mathrm{ct}} - E_{\mathrm{eq}} \tag{9a}$$

$$E_{\mathrm{ct}} = \Phi_{\mathrm{s,ext}} - \Phi_{\mathrm{l}} \tag{9b}$$

$$E_{\mathrm{eq}} = E_{\mathrm{eq,ref}}(T) - \left(\frac{RT}{nF}\right) \ln \prod_j \left(\frac{c_j}{c_{j,\mathrm{ref}}}\right)^{v_j} \tag{9c}$$

where $E_{\mathrm{eq,ref}}(T) \left[\mathrm{V}\right]$ is the reference equilibrium potential at temperature T, n is the number of electrons involved in the reaction, $c_{j,\mathrm{ref}} \left[\mathrm{mol\,m^{-3}}\right]$ is the reference concentration, and v_j is the stoichiometric coefficient of species. This relationship ties the electrochemical kinetics to the thermodynamics of the system, enabling a detailed simulation of the electrochemical processes.

The double layer current density is represented in equation (10):

$$i_{\mathrm{dl}} = \left[\left(\frac{\partial(\Phi_{\mathrm{s,ext}} - \Phi_{\mathrm{l}})}{\partial t}\right)\right] C_{\mathrm{dl}} \tag{10}$$

where $\Phi_{\mathrm{s,ext}} \left[\mathrm{V}\right]$ is the electric potential in the solid electrode, $\Phi_{\mathrm{l}} \left[\mathrm{V}\right]$ is the electric potential in the electrolyte, and $C_{\mathrm{dl}} \left[\mathrm{F\,m^{-2}}\right]$ is the double layer capacitance. This term accounts for the capacitive behavior at the electrode–electrolyte interface, which is important for modeling the transient response of the system.

Solid mechanics physics

Solid mechanics physics was used to describe the mechanical behavior of IPMCs, such as stress, strain, and deformation. In previous studies of IPMC actuation [24, 25], the solid mechanics physics interface plays an important role in computing the body load caused by ion migration and associating it with the displacement of the domains. In the present study, this physics interface was incorporated to examine the potential influence of tensile loading on cation mobility, since microcracks are typically formed under loads and deformation of IPMC. The equation governing in the solid mechanics interface is given as below:

$$\rho\left(\frac{\partial^2 u}{\partial t^2}\right) = \nabla \cdot S + F_{\mathrm{v}} \tag{11}$$

where $\rho \left[\mathrm{kg\,m^{-3}}\right]$ is the material density, $u \left[\mathrm{m}\right]$ is the displacement vector, $S \left[\mathrm{Pa}\right]$ is the stress tensor, and $F_{\mathrm{v}} \left[\mathrm{N\,m^{-3}}\right]$ is the body load density, representing the volumetric forces acting on the body. The stress tensor is derived from the material's response to mechanical loads and includes contributions from both external forces and internal stresses because of ion migration. The top edge of the model was fixed by adding a fixed constraint boundary condition, and the load was applied by adding a boundary load boundary condition. The boundary load condition is given as following.

$$S \cdot n = F_{\mathrm{A}} \tag{12}$$

where S is stress, n is the normal vector to the boundary, and $F_{\mathrm{A}} \left[\mathrm{N\,m^{-2}}\right]$ is the traction vector on the boundary.

2.3.3. Cyclic voltammogram and specific capacitance. The cyclic voltammograms of IPMC models were obtained using cyclic voltammetry study module, and the specific capacitance ($C_{\mathrm{sp}} \left[\mathrm{F\,g^{-1}}\right]$) was calculated using equation (13),

$$C_{\mathrm{sp}} = \int \frac{I(\mathrm{V})\ \mathrm{d}V}{mv\Delta V} \tag{13}$$

where I [A] is the current, $m \left[\mathrm{g}\right]$ is the mass of active material, $v \left[\mathrm{V\,s^{-1}}\right]$ is scan rate, and $\Delta V \left[\mathrm{V}\right]$ is the potential window.

3. Results and discussion

3.1. Ion distribution

Figure 2 shows the cation concentration distribution within the IPMC membrane domain at different times points to verify that the concentration distribution aligns with experimental results. The ion transport occurs only in the Nafion™ membrane, as the electrodes are excluded from this computation because no charged species migrate within the platinum

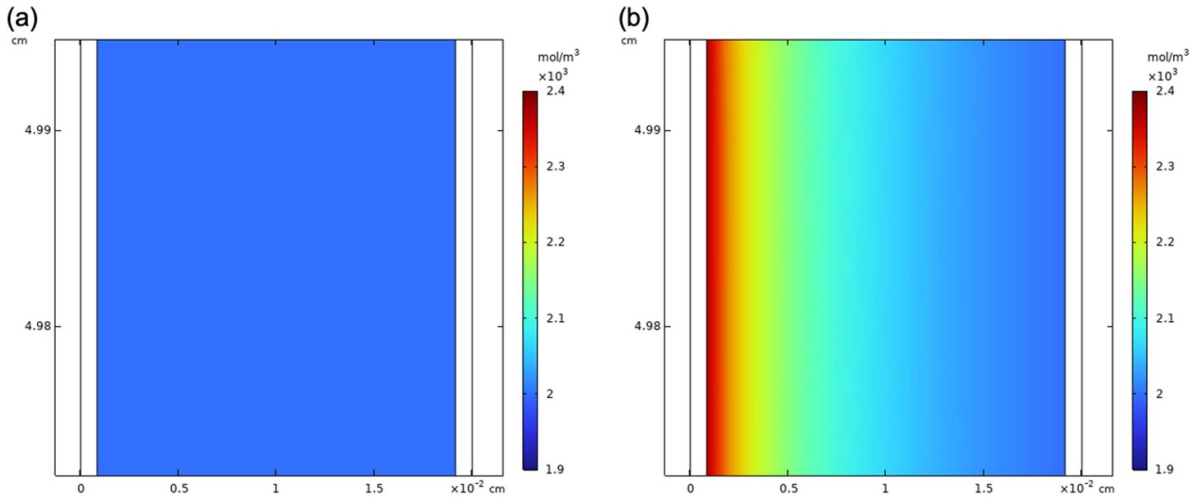

Figure 2. Ion distribution in the membrane domain of defect-free IPMC model at 0 s (a) and 73.315 s (b). The scan rate is 0.015 V s^{-1}.

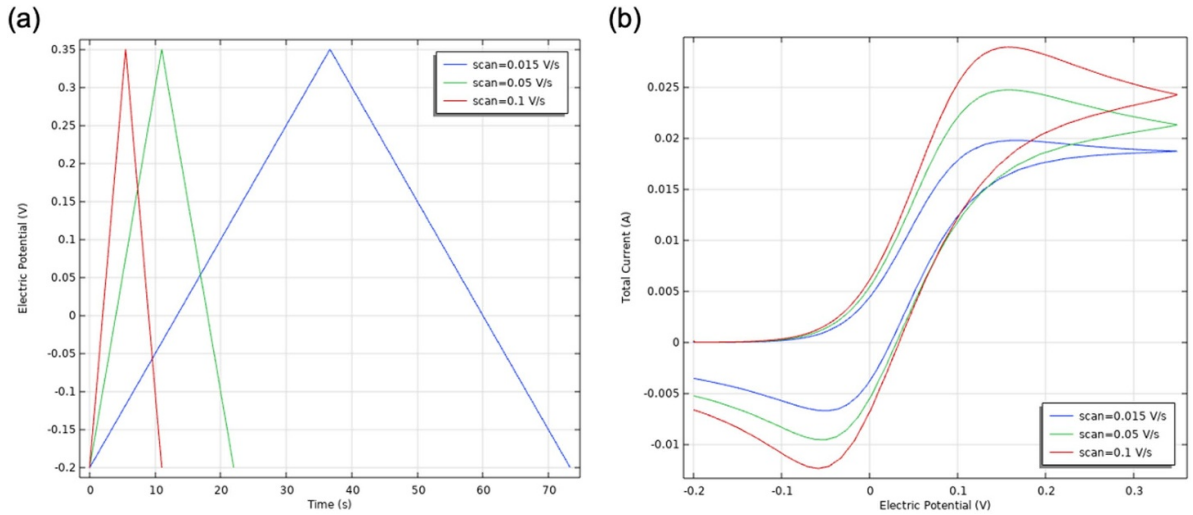

Figure 3. Cyclic voltammetry (CV) characterization of the IPMC model at different scan rates. (a) Triangular potential sweep from −0.2 V to 0.35 V at scan rates of 0.015, 0.05, and 0.1 V s^{-1}. (b) Cyclic voltammogram (current vs. potential) at different scan rates.

domain. Initially, a uniform concentration of 2000 mol m^{-3} of cations is set across the membrane domain, as shown in figure 2(a). At ∼73 s, with a scan rate of 0.015 V s^{-1}, a negative voltage (∼−0.2 V) is applied to the left electrode, causing positively charged cations to electrostatically move towards the negative electrode (figure 2(b)). This behavior is consistent with the experimental observation and IPMC principles, in which ions respond to electric potential [2, 27]. The cations migrate towards the cathode, causing an accumulation that results in a depleted concentration at the anode. Capturing this migration and redistribution of ions is important for validating the simulation against experimental data.

3.2 Effects of scan rate

The scan rate directly influences the shape and magnitude of the cyclic voltammetry (CV) response. Figure 3 shows cyclic voltammograms of the IPMC model at various scan rates. At a low scan rate of 0.015 V s^{-1}, the gradual voltage change provides sufficient time for the ions within the IPMC to migrate and redistribute in response to the imposed electric field, resulting in a gradual increase of current. The slow scan rate also enhances the ability of the IPMCs to reach near equilibrium states at each step of the voltage cycle. Consequently, the current density response exhibits a peak corresponding to the redox reactions at the electrodes, indicating efficient ion migration and reaction kinetics.

As the scan rate increases, ion redistribution becomes limited. The current response peaks are narrower compared to the one observed at 0.015 V s^{-1}, indicating reduced ion mobility and incomplete equilibration. At the highest scan rate of 0.1 V s^{-1}, the applied potential changes too rapidly for ions to fully migrate and respond to the applied voltage sweep, emphasizing resistive rather than capacitive behavior. The resulting CV curve shows narrower peaks, indicating the electrochemical reactions and ion migration processes are kinetically limited.

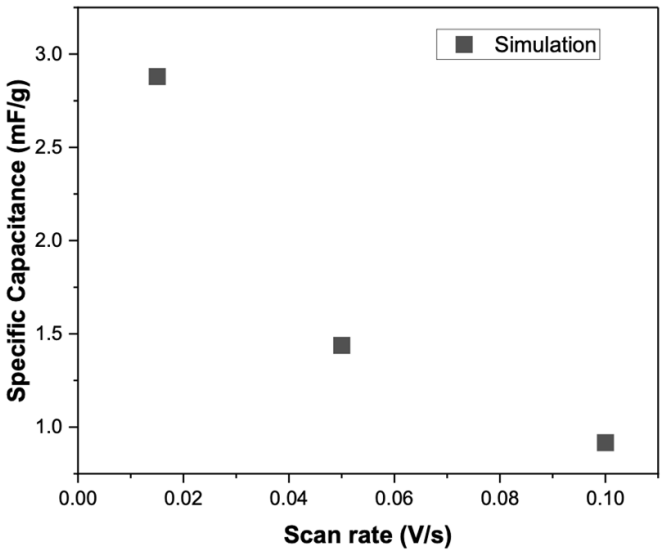

Figure 4. Specific capacitance at difference scan rates.

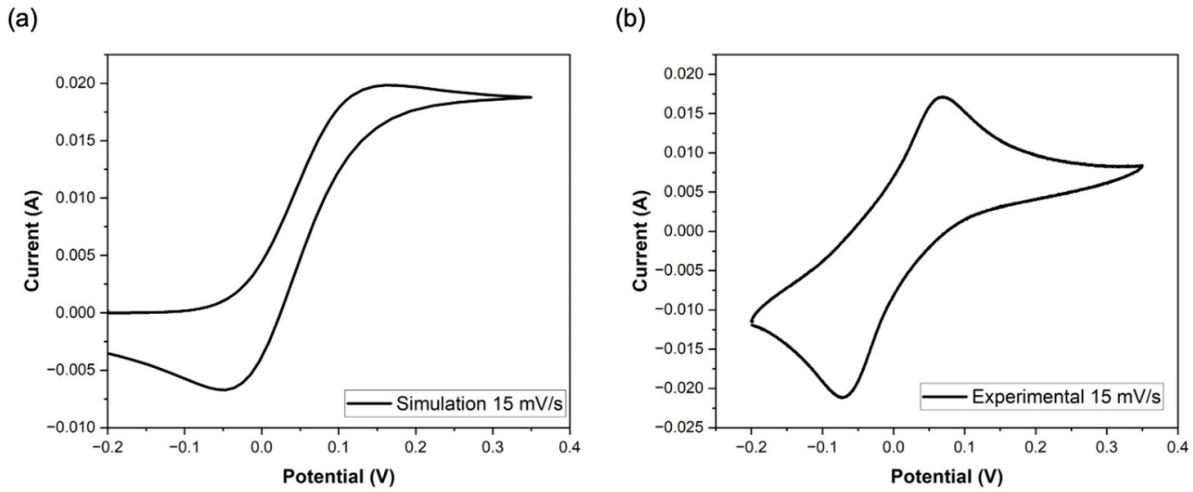

Figure 5. Cyclic voltammogram of IPMC at a scan rate of 0.015 V s^{-1} obtained from simulation (a) and experiment (b).

The scan rate also influences the specific capacitance. The specific capacitance is larger at lower scan rate, as shown in figure 4. The slow scan rate enhances the ability of the IPMCs to reach near equilibrium states at each step of the voltage cycle, allowing the capacitive double layer to charge and discharge more effectively. In contrast, at high scan rates, specific capacitance is smaller as ion mobility is limited, and polarization is delayed. This behavior reflects the dynamic interplay between scan rate and ion migration kinetics within the membrane domain and highlights the importance of scan rate when evaluating charge storage mechanisms in IPMC capacitors [28].

3.3. Comparison between simulated and experimental CVs

The cyclic voltammetry curve at 0.015 V s^{-1} scan rate, obtained from COMSOL simulation, is compared with the experimental result in figure 5. The simulated CV curve is narrower than the experimental one, resulting in the calculated specific capacitance of 2.88 mF g^{-1}, whereas the experiment value is 6.68 mF g^{-1}. This discrepancy indicates that the model underestimates the capacitive behavior of the IPMC, which is likely due to modeling simplifications, including the exclusion of porous electrode structures and the complex interpenetrating morphology at the membrane–electrode interface, both known to enhance electrochemical performance by increasing effective surface area and ion accessibility [2, 22, 29]. Nonetheless, the simulation captures key qualitative features of the experimental CV curve, such as the overall shape and current scale, suggesting that the model reasonably reflects the electrochemical behavior of IPMC capacitors. This qualitative agreement supports the model's applicability for comparative analyses, particularly in analyzing relative performance changes under different operational conditions or structural modifications such as electrode cracking and mechanical loading.

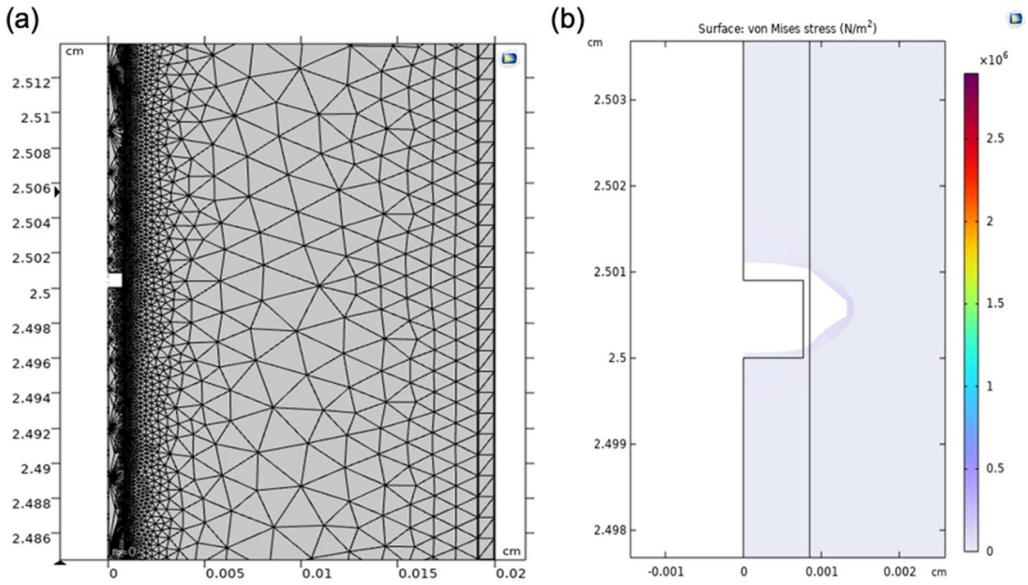

Figure 6. Modeling of single microcrack in the IPMC electrode. (a) Finite element mesh showing local refinement near the cracked electrode. (b) Stress distribution around the crack.

While the influence of electrode porosity is acknowledged, it was intentionally excluded from the present model to reduce computational complexity and isolate the effects of electrode cracking. Modeling a porous electrode would require more detailed geometrical representation and additional physics to capture ion transport within a heterogeneous network, which was beyond the scope of this foundational study. The goal here was to develop a computationally efficient framework capable of capturing key electrochemical behavior and enabling relative performance comparison under different structural conditions. In addition, the use of idealized or literature-based material parameters, such as ion diffusion coefficients and membrane permittivity, may contribute to the quantitative discrepancy. For example, a lower diffusion coefficient would reduce ion mobility and suppress current response, resulting in lower apparent capacitance. The model was not intended to reproduce exact experimental values but rather to capture qualitative trends and evaluate the influence of structural features such as microcracks.

3.4. Effects of cracks and mechanical loading

The electrochemical performance of the IPMC with cracked electrodes is investigated in this section. To incorporate cracks, the original IPMC model was modified by introducing a single rectangular-shaped microcrack at the center of one of the electrodes, as shown in figure 6. The rectangular shape was chosen as a representative based on a prior modeling work, which showed that rectangular cracks exerted a more pronounced influence on IPMC actuation behavior than U- or V-shaped cracks [21]. Although that study focused on actuation, both actuation and capacitive behavior in IPMC originate from the same electrochemical transduction process involving ion migration and charge redistribution. While the rectangular shape may not fully represent the morphological variability of experimentally observed electrode damage [20], it provides a conservative approximation to evaluate the effects of microcracks on capacitive performance. The mesh near the electrodes was automatically refined using the physics-controlled mesh settings, resulting in smaller elements near the electrode boundary and within the electrode.

Firstly, the influence of tensile loading was investigated, as a load applied parallel to the electrode surfaces elongates the IPMC and induce the formation of microcracks in the electrodes [20]. Figure 6(b) shows the stress concentration around the single microcrack in the electrode. Although there is a higher local stress around the crack, the stress is normalized outside the immediate microcrack. The absence of significant stress concentrations outside the microcrack implies that the structural integrity of the IPMC remains largely intact. This suggests that the presence of a single microcrack, along with substituent tension loadings, would not result in substantial changes to the electrical performance of the IPMC, as it is closely related to the uniform distribution and movement of ions within the polymer membrane. Since the stress concentration around the microcrack is minimal, ion migration and associated electrical characteristics are likely not significantly disrupted. The negligible impact of microcracks is also shown in IPMC with multiple cracks. Figure 7 shows concentration profiles without cracks and with 15 microcracks. The concentration drops from the left electrode is remarkably similar. This outcome suggests the presence of multiple microcracks does not drastically alter the overall ion distribution within the IPMC. This similarity in ion concentration gradients can be attributed to the nature of ion transport in the polymer membrane. Despite the presence of microcracks, the polymer network still provides sufficient pathways for ions to migrate effectively.

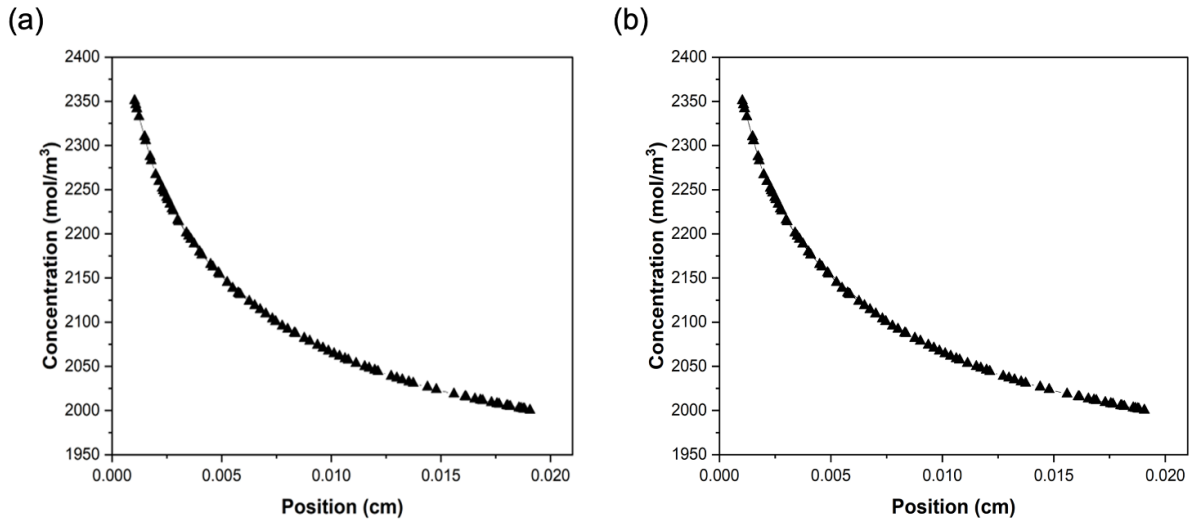

Figure 7. Comparison of the concentration profiles from the left electrode in IPMC models without cracks (a) and with 15 cracks, at 73.312 s under a scan rate of 0.015 V s^{-1}.

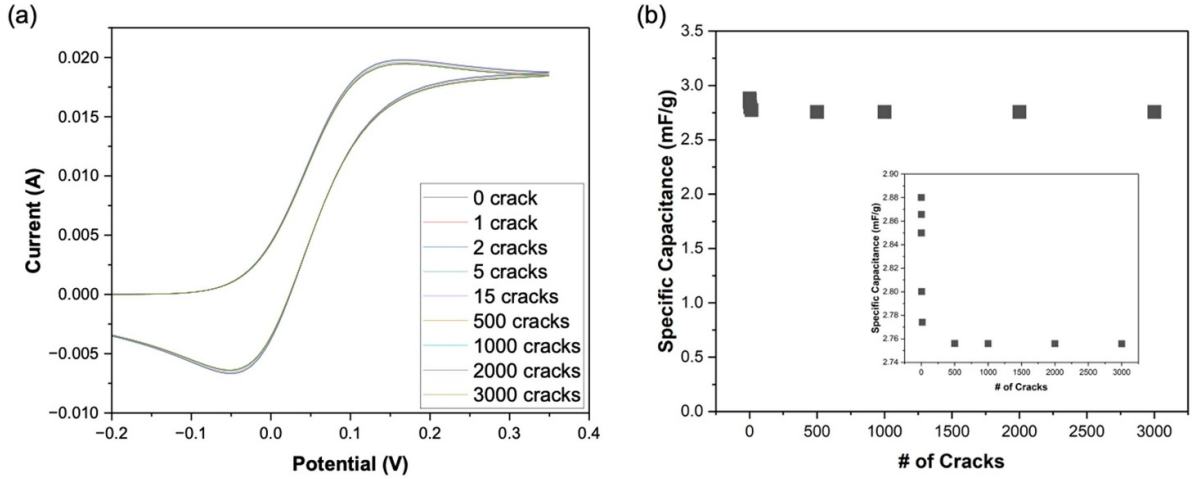

Figure 8. Cyclic voltammograms (a) and specific capacitance (b) of IPMC models with various number of microcracks.

The performance of IPMC was further studied by introducing various number of microcracks, ranging from 0 to 3000 in figure 8. It should be noted that the microcracks were introduced into the model at random to reflect the unpredictable nature of crack formation observed experimentally [20]. The choice of 3000 cracks is based on observations from SEM images which indicated an average of 6–10 microcracks per 100 μms [20]. The CV curves of IPMC models with various number of cracks (figure 8(a)) exhibited minimal changes as the number of cracks increased. Specifically, the plots showed minor variations in peak shapes, indicating the minor impact of microcracks on the ion transport. This is likely because the microcracks are relatively small compared to the overall dimensions of the IPMC and do not create sufficiently large discontinuities to disrupt the overall ion flow. Instead, the ions can bypass these minor defects and continue to migrate towards the electrode, maintaining uniform concentration gradient.

The specific capacitance also showed a small reduction, from ∼2.88 mF g^{-1} to 2.75 mF g^{-1} (figure 8(b)). This suggests that the microcracks disrupt the continuity of ion transport pathways and increase the internal resistance within the material. In other words, the gaps created by the microcracks reduce the effective electrode contact with the membrane, reducing electrochemical reactions and leading to lower current densities and consequently a decrease in capacitance. However, this change is relatively minor (∼4.5%) and suggests that the presence of microcracks does not drastically impair capacitive performance. Interestingly, most of the capacitance decline occurs with the initial introduction of a small number of cracks (below ∼500), after which the values plateau and remain nearly constant even as the crack number increases further. This trend indicates a saturation effect: once a critical crack density is reached, additional cracks have a negligible effect on capacitance.

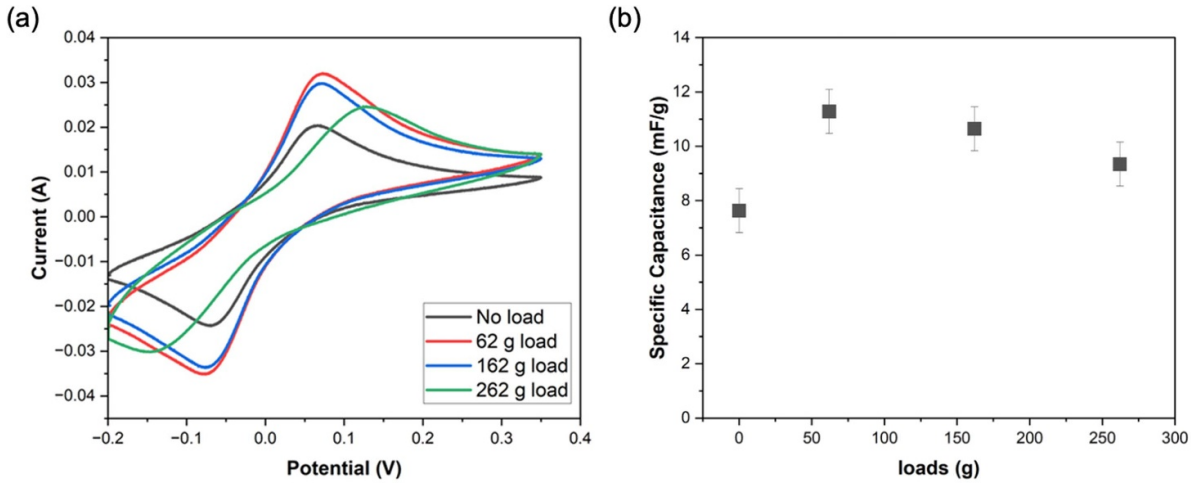

Figure 9. Experimentally measured cyclic voltammograms (a) and corresponding specific capacitance (b) of IPMC strips under various tensile loads.

Figure 9 shows the experimental CV curves and specific capacitance values under various loadings. The specific capacitance initially increases under light load and then decreases slightly. Based on the previous discussion about the effect of loading and microcracks, the initial increase is thought to be attributed to the mechanical activation and alignment of conductive pathways and possibly improved electrode contact, enhancing the initial ion migration and electrochemical activity. As loading increased, the specific capacitance decreases, likely due to the formation of additional cracks, as supported by the simulation results. The cumulative impact of numerous microcracks may disrupt the continuity of the ion transport pathways. However, the reduction in the electrochemical performance is not significant in both simulation and experimental results.

4. Concluding remarks

This work focused on the modeling of IPMC capacitors using COMSOL multiphysics, emphasizing the development of a simulation framework and the investigation of the electrochemical behavior of IPMCs, as well as the effects of microcracks in the electrodes on the electrical performance of IPMC. The simulated cyclic voltammetry curves of IPMC model and ion distribution showed qualitative agreement with experimental data, with potential improvements possible through the incorporation of a porous electrode structure. Additionally, the model was used to study the influence of microcracks, particularly how cracks in electrodes affect ion transport and specific capacitance. Based on the model and simulation results, the overall findings indicate that even with a large number of randomly distributed microcracks (6–10 microcracks per 100 μm), the reduction in specific capacitance was modest ($\sim$4.5%), suggesting that the performance degradation remained relatively minor. Although incorporating more realistic electrode geometry and conducting parametric studies are necessary to validate the generality of this trend, the results suggest that IPMCs can tolerate structural imperfections without significant losses in electrochemical performance. This robustness is advantageous for long-term reliability of IPMC-based energy storage devices, as minor mechanical damage does not drastically affect functionality. While this study adopts a simplified electrode structure and considers only rectangular-shape crack geometry, the framework lays groundwork for future investigations. Further studies incorporating porous electrode dynamics and exploring diverse crack geometries would improve predictive accuracy and broaden the model's applicability.

Data availability statement

All data that support the findings of this study are included within the article (and any supplementary files).

Acknowledgment

This work was supported in part by the U.S. Department of Energy and the Savannah River National Laboratory under BSRA Contract 000065847500. We also acknowledge partial financial support from the Army Research Office under Award Number W911NF2310180. Additionally, L N gratefully acknowledges the generous support from the Howe Foundation Research Fellowship during her Ph.D. studies.

ORCID iDs

John Albert Faccinto 0009-0007-7820-5945
Kwang J Kim 0000-0003-2134-4964

References

[1] Bar-Cohen Y, Leary S, Shahinpoor M, Harrison J and Smith J 1999 Electroactive polymer (EAP) actuators for planetary applications electroactive polymer actuators and devices (EAPAD) *Smart Structures and Materials 1999: Electroactive Polymer Actuators and Devices* (*Newport Beach, CA, United States*, *28 May 1999*) vol 3669 *1999 Symposium on Smart Structures and Materials* (SPIE) pp 1–7

[2] Shahinpoor M and Kim K J 2001 Ionic polymer-metal composites: i. Fundamentals *Smart Mater. Struct.* **10** 819

[3] Zhang H, Lin Z, Hu Y, Ma S, Liang Y, Ren L and Ren L 2023 Low-voltage driven ionic polymer-metal composite actuators: structures, materials, and applications *Adv. Sci.* **10** 2206135

[4] Bhandari B, Lee G-Y and Ahn S-H 2012 A review on IPMC material as actuators and sensors: fabrications, characteristics and applications *Int. J. Precis. Eng. Manuf.* **13** 141–63

[5] He Q, Yin G, Vokoun D, Shen Q, Lu J, Liu X, Xu X, Yu M and Dai Z 2022 Review on improvement, modeling, and application of ionic polymer metal composite artificial muscle *J. Bionic Eng.* **19** 279–98

[6] Jung K, Nam J and Choi H 2003 Investigations on actuation characteristics of IPMC artificial muscle actuator *Sens. Actuators A* **107** 183–92

[7] Anand S V, Arvind K, Bharath P and Roy Mahapatra D 2010 Energy harvesting using ionic electro-active polymer thin films with Ag-based electrodes *Smart Mater. Struct.* **19** 045026

[8] Patel S N and Mukherjee S 2022 Manufacturing, characterization and experimental investigation of the IPMC shoe energy harvester *J. Braz. Soc. Mech. Sci. Eng.* **44** 42

[9] Tiwari R and Kim K J 2013 IPMC as a mechanoelectric energy harvester: tailored properties *Smart Mater. Struct.* **22** 015017

[10] Aureli M, Lin W and Porfiri M 2009 On the capacitance-boost of ionic polymer metal composites due to electroless plating: theory and experiments *J. Appl. Phys.* **105** 104911

[11] Bhattacharyya T K, Mondal M and Datta A 2021 Ipmc based flexible platform: a boon to the alternative energy solution *Management and Applications of Energy Storage Devices* ed K E Okedu (IntechOpen) (https://doi.org/10.5772/intechopen.99434)

[12] Napollion L and Kim K J 2024 Ionic polymer-metal composite (IPMC) as a flexible capacitor: an experimental study *Smart Mater. Struct.* **33** 125009

[13] He Q, Yu M, Yang X, Kim K J and Dai Z 2015 An ionic electro-active actuator made with graphene film electrode, chitosan and ionic liquid *Smart Mater. Struct.* **24** 065026

[14] He Y, Chen W, Gao C, Zhou J, Li X and Xie E 2013 An overview of carbon materials for flexible electrochemical capacitors *Nanoscale* **5** 8799–820

[15] Wang Y, Zhu Z, Chen H, Luo B, Chang L, Wang Y and Li D 2014 Effects of preparation steps on the physical parameters and electromechanical properties of IPMC actuators *Smart Mater. Struct.* **23** 125015

[16] Lee S-G, Park H-C, Pandita S D and Yoo Y 2006 Performance improvement of IPMC (ionic polymer metal composites) for a flapping actuator *Int. J. Control Autom. Syst.* **4** 748–55 (available at: https://www.ijcas.org/journal/view.html?pn=myread&uid=429&vmd=Full#n)

[17] Shahinpoor M 2015 *Fundamentals of Ionic Polymer Metal Composites (IPMCS) In Ionic Polymer Metal Composites (IPMCS): Smart Multi-Functional Materials and Artificial Muscles* (The Royal Society of Chemistry) pp 1–60

[18] Johanson U, Punning A and Aabloo A 2015 *Ionic Polymer Metal Composites with Electrochemically Active Electrodes in Ionic Polymer Metal Composites (IPMCS): Smart Multi-Functional Materials and Artificial Muscles* (The Royal Society of Chemistry) pp 215–27

[19] Tiwari R and Kim K 2008 Improved IPMC sensing by use of cation and through induced nano-to-micro scale surface cracks *Sensors and Smart Structures Technologies for Civil, Mechanical, and Aerospace Systems* (*San Diego, California, United States*, *8 April 2008*) *SPIE Smart Structures and Materials + Nondestructive Evaluation and Health Monitoring* vol 6932 (SPIE) pp 1057–68

[20] Napollion L and Kim K J 2023 Electrochemical performance of ionic polymer metal composite under tensile loading *Smart Mater. Struct.* **32** 095025

[21] Swain P K, Shekh M J and Swarrup J S 2021 Modelling the effect of crack formation on the actuation behaviour of ionic polymer metal composite *Int. J. Nanotechnol.* **18** 763–75

[22] Onishi K, Sewa S, Asaka K, Fujiwara N and Oguro K 2001 Morphology of electrodes and bending response of the polymer electrolyte actuator *Electrochim. Acta* **46** 737–43

[23] Kim K J and Shahinpoor M 2003 Ionic polymer-metal composites: II. Manufacturing techniques *Smart Mater. Struct.* **12** 65–79

[24] Pugal D, Kim K J and Aabloo A 2011 An explicit physics-based model of ionic polymer-metal composite actuators *J. Appl. Phys.* **110** 084904

[25] Pugal D, Stalbaum T, Palmre V and Kim K J 2015 Modeling ionic polymer metal composites with COMSOL: step-by-step guide *Ionic Polymer Metal Composites (IPMCS): Smart Multi-Functional Materials and Artificial Muscles* (The Royal Society of Chemistry) pp 185–214

[26] Chinnasa P, Ponhan W and Choawunklang W 2019 Modeling and simulation of a $LaCoO_3$ nanofibers /CNT electrode for supercapacitor application *J. Phys.: Conf. Ser.* **1380** 012101

[27] Park I-S, Kim S-M, Pugal D, Huang L, Tam-Chang S-W and Kim K J 2010 Visualization of the cation migration in ionic polymer-metal composite under an electric field *Appl. Phys. Lett.* **96** 043301

[28] Md Jamil F, Sulaiman M A, Mohd Ibrahim S, Masrom A K and Yahya M Z A 2016 Effects of different electrolyte concentrations and scan rates in mesoporous carbon electrode-based capacitance *Adv. Mater. Res.* **1133** 3–7

[29] Wang Y, Liu J, Zhu Y, Zhu D and Chen H 2017 Formation and characterization of dendritic interfacial electrodes inside an ionomer *ACS Appl. Mater. Interfaces* **9** 30258–62